Tau isoform expression and phosphorylation in marmoset brains

Received for publication, March 12, 2019, and in revised form, May 23, 2019 Published, Papers in Press, June 5, 2019, DOI 10.1074/jbc.RA119.008415

Govinda Sharma[‡1,2], Anni Huo[‡1], Taeko Kimura[‡§], Seiji Shiozawa[¶], Reona Kobayashi[¶‖], Naruhiko Sahara[§], Minaka Ishibashi[**], Shinsuke Ishigaki[**], Taro Saito[‡], Kanae Ando[‡], Shigeo Murayama[‡‡], Masato Hasegawa[§§], Gen Sobue[**], Hideyuki Okano[¶‖], and Shin-ichi Hisanaga[‡§§3]

From the [‡]Laboratory of Molecular Neuroscience, Faculty of Sciences, Tokyo Metropolitan University, Minami-osawa, Hachioji, Tokyo 192-0397, Japan, the [§]Department of Functional Brain Imaging Research, National Institute of Radiological Sciences, 4-9-1 Anagawa, Inage, Chiba, Chiba 263-8555, Japan, the [¶]Department of Physiology, School of Medicine, Keio University, Shinjuku, Tokyo 160-8582, Japan, the [‖]Laboratory for Marmoset Neural Architecture, RIKEN Center for Brain Science, Wako, Saitama 351-0198, Japan, the [**]Research Division of Dementia and Neurodegenerative Disease, Nagoya University Graduate School of Medicine, Nagoya, Aichi 466-8550, Japan, the [‡‡]Tokyo Metropolitan Institute of Gerontology, Itabashi, Tokyo 173-0015, Japan, and the [§§]Tokyo Metropolitan Institute of Medical Science, Setagaya, Tokyo 156-8506, Japan

Edited by Paul E. Fraser

Tau is a microtubule-associated protein expressed in neuronal axons. Hyperphosphorylated tau is a major component of neurofibrillary tangles, a pathological hallmark of Alzheimer's disease (AD). Hyperphosphorylated tau aggregates are also found in many neurodegenerative diseases, collectively referred to as "tauopathies," and tau mutations are associated with familial frontotemporal lobar degeneration (FTLD). Previous studies have generated transgenic mice with mutant tau as tauopathy models, but nonhuman primates, which are more similar to humans, may be a better model to study tauopathies. For example, the common marmoset is poised as a nonhuman primate model for investigating the etiology of age-related neurodegenerative diseases. However, no biochemical studies of tau have been conducted in marmoset brains. Here, we investigated several important aspects of tau, including expression of different tau isoforms and its phosphorylation status, in the marmoset brain. We found that marmoset tau does not possess the "primate-unique motif" in its N-terminal domain. We also discovered that the tau isoform expression pattern in marmosets is more similar to that of mice than that of humans, with adult marmoset brains expressing only four-repeat tau isoforms as in adult mice but unlike in adult human brains. Of note, tau in brains of marmoset newborns was phosphorylated at several sites associated with AD pathology. However, in adult marmoset brains, much of this phosphorylation was lost, except for Ser-202 and Ser-404 phosphorylation. These results reveal key features of tau expression and phosphorylation in the marmoset brain, a potentially useful nonhuman primate model of neurodegenerative diseases.

Tau is a microtubule (MT)[4]-associated protein expressed primarily in the axons of mammalian neurons (1–4). Tau also constitutes a major component of the neurofibrillary tangles (NFTs) found in neurons of brains of Alzheimer's disease (AD) patients. Tau is a naturally unfolded protein composed of an N-terminal projection domain and C-terminal region containing MT-binding (MTB) repeats. There are six isoforms of tau, which are generated by alternative splicing of N-terminal insertions (exons 2/3) and the C-terminal second MTB repeat (exon 10) from a single gene. In particular, splicing out or in from exon 10 gives rise to three-repeat (3R) or four-repeat (4R) tau with different MT-binding activities. This splicing is regulated developmentally (5), and an imbalance between 3R and 4R tau is found in AD (3). However, the molecular mechanisms of this splicing and its significance are not fully understood.

The MTB and MT assembly activities of tau are regulated by phosphorylation (4, 6, 7). Tau in NFTs is hyperphosphorylated (8–11), and aggregates of hyperphosphorylated tau are also detected in many neurodegenerative diseases, which are collectively referred to as "tauopathies" (2–4). The immunostaining of NFTs with several anti-phospho-tau antibodies is routinely employed to provide a final diagnosis of AD or other tauopathies (12, 13), but the significance of tau phosphorylation for the development of AD or tauopathies is not yet clear. This is because of the difficulty of studying the phosphorylation states of tau in human brains. Most previous studies have used autopsy human brain samples with long post-mortem interval (PMI), during which tau undergoes dephosphorylation. In fact, tau in mouse brain is shown to be dephosphorylated quickly at a number of sites after sacrifice (16). We recently examined in detail the phosphor-

This work was supported in part by a MEXT Grant-in-aid project, Scientific Research on Innovation Area (Brain Protein Aging and Dementia Control) of Japan 26117004 (to S. H.), and by MEXT Grants-in-aid 16K07060 (to S. H.) and 60748820 (to T. K.). The authors declare that they have no conflicts of interest with the contents of this article.

This article contains Figs. S1–S4.

[1] Both authors contributed equally to this work.

[2] Present address: Faculty of Veterinary Medicine, University of Calgary, Alberta T2N 1N4, Canada.

[3] To whom correspondence should be addressed: Dept. of Biological Sciences, Graduate School of Science, Tokyo Metropolitan University, Minami-Osawa, Hachioji, Tokyo 192-0397, Japan. Tel.: 81-42-677-2754; Fax: 81-42-677-2559; E-mail: hisanaga-shinichi@tmu.ac.jp.

[4] The abbreviations used are: MT, microtubule; 3R, three-repeat; 4R, four-repeat; AD, Alzheimer's disease; FTLD, frontotemporal lobar degeneration; ISM, intron-splicing modulator; ISS, intron-splicing silencer; MTB, MT-binding; NFT, neurofibrillary tangle; PMI, post-mortem interval; P, postnatal day; AEBSF, 4-(2-aminoethyl)-benzenesulfonyl fluoride hydrochloride.

ylation of tau in human brains, both for normal control and AD patients with 3–4 h of shortest PMI (14) by Phos-tag phosphoaffinity electrophoresis (15). There was abundant nonphosphorylated tau in human brains. In contrast, tau in biopsy brain samples taken from live humans is phosphorylated more than tau in postmortem autopsy samples (17). However, the effect of anesthesia was not considered at that time. It has been recently shown that anesthesia increases tau phosphorylation (18). Therefore, the exact *in vivo* phosphorylation states of tau in human brains are not yet satisfactorily uncovered.

Rodents have alternatively been used for the analysis of *in vivo* tau phosphorylation (8, 19, 20). They might have provided useful information implicating the phosphorylation of tau in human brains, but there are arguments that rodents do not necessarily serve as a proper model of tauopathies, which develop in aged individuals. The life span of rodents is much shorter than that of humans. The isoform expression of mouse tau is different from that of humans. Whereas 3R and 4R tau are expressed in adult human brains, only 4R tau is expressed in adult mouse brains (21–24). Further, the hyperphosphorylation and aggregation of tau do not occur in mouse brains. The desirable model is that of the nonhuman primate (25), which captures the pathological features of tau observed in humans. The common marmoset (*Callithrix jacchus*), a New World monkey, is poised as a nonhuman primate model for age-dependent neurodegenerative diseases (26, 27). Compared with other nonhuman primates, such as macaque and rhesus monkeys, marmosets are easy to house and handle due to their small size of ~300 g and have a relatively short life span with a maximum age of 16–18 years (25). Moreover, it is possible to manipulate the genes of marmosets (28). In fact, marmosets have already been used as the model of 1-methyl-4-phenyl-1,2,3,6-tetrahydropyridine (MPTP)-induced Parkinson disease and age-dependent accumulation of α-synuclein, for example (29, 30). We also used marmosets in a study on the propagation of α-synuclein aggregates (31). Before using animals as a model, however, it is useful to identify the properties of the target protein (*e.g.* tau in the case of tauopathies). To our surprise, however, no biochemical work has been conducted on tau proteins in marmoset brains.

In this study, we isolated tau cDNA from marmoset brains and investigated the expression of tau isoforms and phosphorylation, two important properties of tau related to AD pathology. Unexpectedly, we found that marmoset tau resembled mouse tau more than human tau in isoform expression.

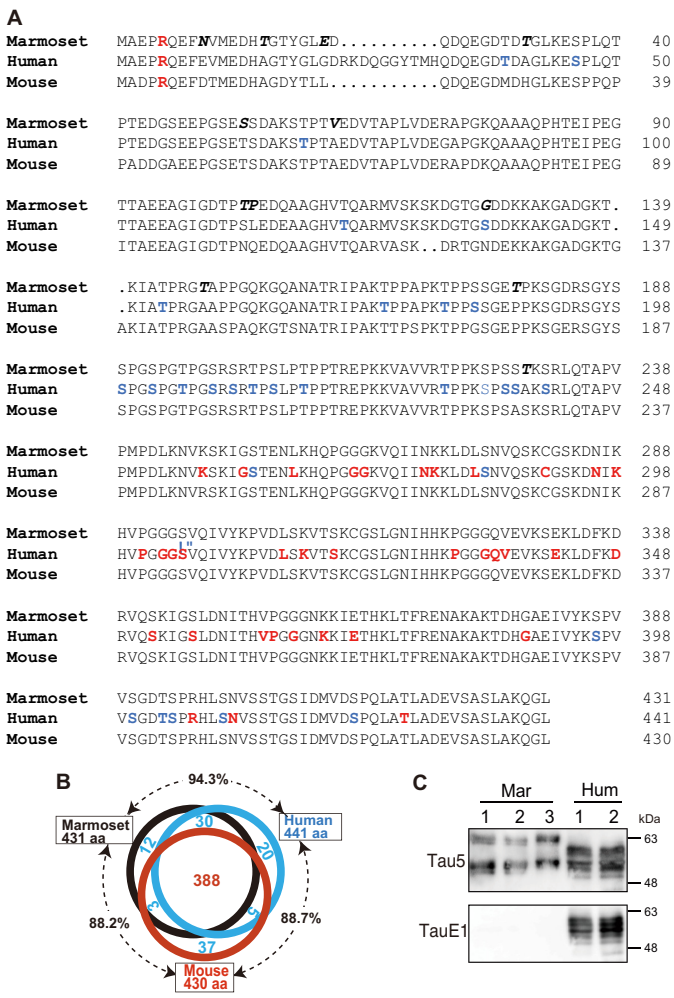

Figure 1. Comparison of amino acid sequences of marmoset tau with human and mouse tau. *A*, amino acid alignment of marmoset tau with human and mouse tau. Amino acids unique to marmoset tau are indicated by *italic boldface type*, FTLD-tau mutation sites are indicated by *red*, and major phosphorylation sites are indicated by *blue*. *B*, homology of amino acid sequences of marmoset tau with human or mouse tau. The total number of amino acids found in marmoset 2N4R tau is 431, which is 10 amino acids shorter than that found in human tau and one amino acid longer than that found in mouse tau. The amino acid identity of marmoset tau and human tau is 94.3%, and that for mouse tau is 88.2%. The three species share 388 of the same amino acids. The number of amino acids that are the same between each pair of species as well as those unique among the three species are denoted in *blue*, and the number of amino acids common to all three species is denoted in *red*, respectively. *C*, immunoblots of marmoset and human tau with Tau5 recognizing common mammalian tau (*top*) and TauE1 specific to human tau (*bottom*).

Results

Marmoset tau is phylogenically distinct from the tau of human and Old World monkeys

The predicted amino acid sequence of marmoset tau can be obtained from the NCBI database (XP_017827929.1). The number of amino acids of this tau is 851, which may be constructed from all exons in the tau gene and is larger than high-molecular weight (or big) tau expressed in the peripheral nervous system (32, 33). Tau protein species expressed in the central nervous system are much smaller due to the omission of exons 4a, 6, and 8 (Fig. S1*A*). Thus, there have been no reports describing the amino acid sequence of tau isoforms expressed in marmoset brains. Therefore, we cloned tau cDNA from cDNA libraries of marmoset brains on postnatal day 0 (P0) and of adults (23 months) using 5′ and 3′ primers based on the predicted DNA sequence by PCR (see "Experimental procedures"). 0N3R tau cDNA with no N-terminal insertion and three MTB repeats (3R) was isolated from the cDNA library of a newborn marmoset brain, and 0N4R (no N-terminal insertion and four MTB repeats (4R)) and 2N4R (two N-terminal insertions and 4R) were obtained from that of an adult marmoset brain. The sequence of cloned tau cDNA matched the mRNA sequence deduced from the genome sequence data (XM_017972440.1). The full amino acid sequence of 2N4R marmoset tau is compared with that of human and mouse tau in Fig. 1*A*. In total, 431

amino acids were found, which is 10 amino acids shorter than the 441 amino acids found in human 2N4R tau. Marmoset 2N4R tau exhibited 94.3 and 88.2% identity to the corresponding isoforms of human and mouse tau, respectively, with 12 amino acids unique to marmoset tau and with 388 amino acids common to human and mouse tau (Fig. 1*B*).

Twelve amino acids unique to marmoset tau were found in the N-terminal region (shown in *italic boldface type* in Fig. 1*A*). N-terminal exon 2/3 insertions are indicated as well. The C-terminal 200 amino acids, including the MTB repeats, are exactly the same as those of human tau. The *MAPT* mutation sites, which are found in frontotemporal lobar degeneration (FTLD) with tau-immunoreactive inclusions (FTLD-tau) (34), previously referred to as FTDP-17 (frontotemporal dementia and parkinsonism linked to chromosome 17) (2–4), were conserved in marmoset tau (shown in *red* in Fig. 1*A*). Major physiological and pathological phosphorylation sites were also conserved (shown in *blue* in Fig. 1*A*). Ten fewer amino acids were found in the N-terminal region of marmoset tau, which corresponds to amino acids 23–32 of human 2N4R tau. Interestingly, the missing region overlapped with the 11 amino acids absent in mouse tau, corresponding to amino acids 22–32 of human tau (Fig. 1*A*). The absence of the sequence in marmoset tau was confirmed by immunoblotting with the human-specific tau antibody generated against amino acids 20–38 of human tau (Fig. 1*C*; see "Experimental procedures"). Whereas adult marmoset tau appeared as two separated bands on SDS-PAGE (Fig. 1*C*, *Tau5*), neither band was recognized by the human-specific TauE1 antibody (Fig. 1*C*).

The amino acid alignment and phylogenic tree of mammalian tau have been recently reported (35). In that report, the N-terminal 11-amino acid insertion was defined as the "primate-unique motif" because the sequence was found in chimpanzees and macaques but not in bovines, goats, cats, or rodents (35). However, the sequence was not present in tau of marmosets, although the marmoset is a primate. To determine the evolutional positioning of marmoset tau, we performed an amino acid sequence alignment of mammalian tau by adding the number of mammalian species to the list given by Stefanoska *et al.* (35). Those added are the gorilla, orangutan, gibbon, and baboon as Old World monkeys; the squirrel monkey, night monkey, and capuchin as New World monkeys; the sifaka and lemur as monkeys of prosimians; the cat, panda, and goat as other mammals; and the Tasmanian devil as a marsupial animal. The alignment was performed with N-terminal 120 amino acids of human tau, and the N-terminal 50-amino acid region is shown in Fig. 2*A*. Considerable variation in the region corresponding to amino acids 19–32 of human tau was found, including in the 11-amino acid stretch referred to as the primate-unique motif (Fig. 2*A*, *highlight*). The "primate-unique motif" was found in humans, all Old World monkeys, and Madagascar monkeys, but not in New World monkeys. Among the other mammals, the corresponding sequence was found in dogs, cats, and pandas, whereas mice, rats, goats, and cows did not have the sequence. Cat tau registered in the Ensemble Genome Browser (MAPT-201) encodes the primate-unique motif, different from that in the previous list of Stefanoska *et al.* (35). A phylogenic tree of mammalian tau is shown in Fig. 2*B*. Although levels of bootstrap support were generally low, the phylogenetic relationship was largely consistent with that inferred from larger datasets (36, 37). This finding suggests that New World monkeys, including marmosets, lost that sequence of tau after their separation from Old World monkeys and that mouse/rat and cow/goat lineages also independently lost the corresponding sequence after their separation from other animal groups.

Isoforms of tau expressed in marmoset brains

The expression of tau isoforms changes with brain development. 3R tau is expressed in embryonic and early postnatal days in both humans and mice (21–24, 38). In contrast, whereas both 3R and 4R tau are expressed in adult brains of humans (21, 23), only 4R isoforms are expressed in the brains of adult mice (20, 24, 38). To reveal the isoforms of tau expressed in the marmoset brains, mRNA transcripts of tau were examined by PCR using newborn and adult marmoset brain cDNA libraries as templates with primers encompassing the N-terminal insertion (exons 2/3) or the second repeat of MTB (exon 10) (Fig. S2). With respect to N-terminal insertions, the 0N isoform was amplified predominantly from the newborn cDNA library with faint bands at the sizes expected from the 1N and 2N isoforms (Fig. 3*A*, *P0*). When the adult cDNA library was used as a template, PCR products corresponding to 0N and 2N tau were amplified (Fig. 3*A*, 23 months (*23M*)). We confirmed them to be tau DNA fragments by DNA sequencing, and a weak band above 2N (*asterisk* in Fig. 3*A*) was an artifact including unknown sequence. For the splicing of exon 10, a 3R product was detected as a stronger band in newborn marmosets, whereas a weak band corresponding to 4R tau was also detected (Fig. 3*B*, *P0*). In contrast, 4R tau was exclusively detected in the adult marmoset cDNA library (Fig. 3*B*, *23M*). A faint band above 4R at P0 (*asterisk* in Fig. 3*B*) was again a PCR artifact. The similar results were obtained from another set of primers (Fig. S3). These results indicate that the isoforms of 0N3R and, to a lesser extent, 0N4R tau are expressed in the brains of newborn marmosets, whereas those of 0N4R and 2N4R are expressed in adult marmoset brains at the mRNA level.

Next, we examined the expression of tau isoforms at the protein level by immunoblotting lysates of the cerebral cortex with Tau5, a phosphorylation-independent antibody for total tau (Fig. 4*A*). Adult human and mouse brains at P5 were blotted on the same membrane for comparison. Marmoset tau at 23 months was composed of two groups of bands: major bands at 55 kDa and weaker bands at ~69 kDa. The tau of newborn brains at P0 appeared as a single band in the same position as the major bands of adult marmoset tau, and they displayed the same mobility as those of human and mouse tau, whereas the upper minor band of adult marmoset tau was larger than the larger, faint band of adult human tau (compare the *first* and *third lanes* in Fig. 4*A*).

To identify the isoforms of two band groups in adult marmoset tau, their electrophoretic mobilities were compared with those of recombinant 0N4R and 2N4R marmoset tau expressed in Neuro-2a cells (Fig. 4*B*). Lysates of both the cerebral cortex and hippocampus showed two groups of bands. The upper bands exhibited the same migration patterns as 2N4R tau, and

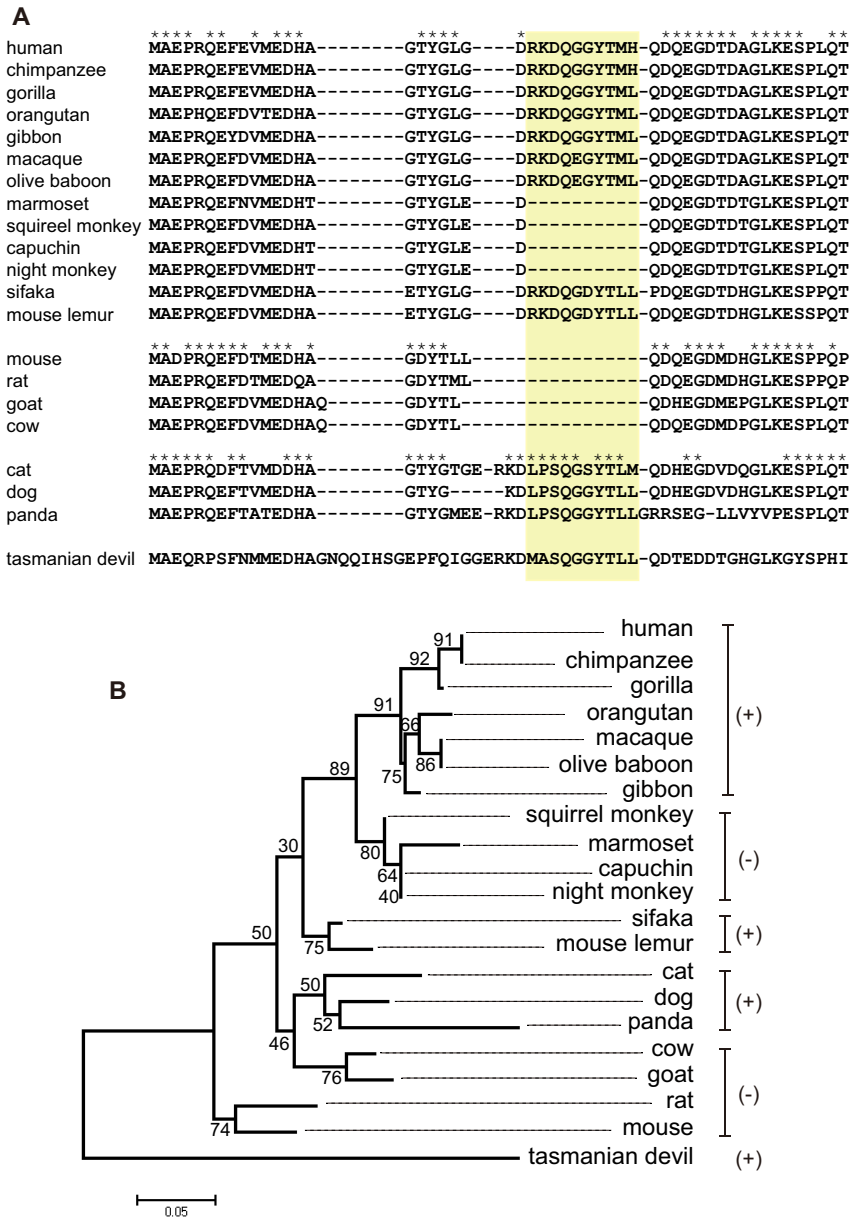

Figure 2. High levels of variability found in amino acid sequences of the N-terminal region of mammalian tau. *A*, amino acid alignment of the N-terminal region of mammalian tau. The N-terminal 50 amino acids of human tau and the corresponding region of other mammalian tau are shown. The upper lineage bloc of species includes primates; humans, apes (the chimpanzee, gorilla, orangutan, and gibbon), and Old World monkeys (the macaque and olive baboon) belong to Catarrhini; New World monkeys (the marmoset, squirrel monkey, capuchin, and night monkey) belong to Platyrrhini; and the sifaka and mouse lemur belong to Strepsirrhini. The second block denotes mice, rats, and other mammals as Rodentia; goats and cows as Ruminantia; and cats, dogs, and pandas as Carnivora. Tasmanian devil tau is shown at the bottom. The sequence defined as the "primate-unique motif" is highlighted. *Asterisks* indicate that the identical amino acids are found in each bloc. *B*, phylogenic tree based on N-terminal 120 amino acids of mammalian tau sequences listed in *A*. Bootstrap values are shown *next to* the branches. The *scale bar* indicates units of the number of amino acid substitutions per site. The presence (+) or absence (−) of the "primate-unique motif" is indicated on the *right*.

the lower bands followed the patterns of 0N4R tau, suggesting that the upper and lower bands of adult marmoset tau are composed of 0N4R and 2N4R isoforms, respectively. Interestingly, the ratio of the upper and lower bands differed among brain regions. The upper band was stronger than the lower band in the cerebellum (Fig. 4*B*, *left*), whereas the ratio of the lower band was much larger in the olfactory bulb than in the hippocampus (Fig. 4*B*, *right*).

As is shown in Fig. 4*A*, 3R and 4R isoforms exhibited the same mobility in SDS-PAGE as those observed for mouse brain tau (20) despite their differing molecular sizes, rendering the definite identification of isoforms difficult, particularly when both isoforms were coexpressed. To determine whether 3R, 4R, or both are expressed at P0 or in adult marmosets, their brain lysates were immunoblotted with 3R (RD3)– and 4R (RD4)–specific antibodies (Fig. 4*C*). Mouse tau at P5 and P60 was used as a reference for 3R and 4R tau, respectively. The blots indicate that both the upper and lower bands in adult marmoset brains were composed of 4R tau, whereas the 3R isoform was predominantly found in newborn marmoset brains in the same position as the lower bands of adult tau by SDS-PAGE (Fig. 4*C* and original blots shown in Fig. S4).

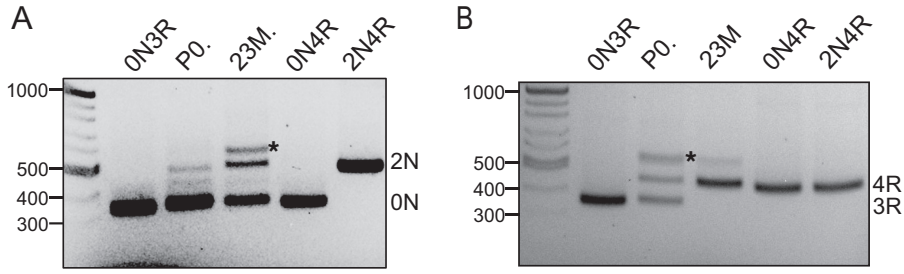

Figure 3. Tau isoforms expressed in newborn and adult marmoset brains. *A* and *B*, agarose gel electrophoresis of the PCR products for exons 2/3 (*A*) and 10 (*B*). The *left side* shows ladder markers of DNA. PCR products of 0N3R, 0N4R, and 2N4R tau plasmids are included as controls of exon 2/3 splicing (*0N* and *2N* in *A*) and exon 10 splicing (*3R* and *4R* in *B*). *P0* and *23M*, PCR products amplified with the cDNA library from newborn (postnatal day 0) and adult (23-month) marmoset brains, respectively. *Asterisks*, unidentified PCR products.

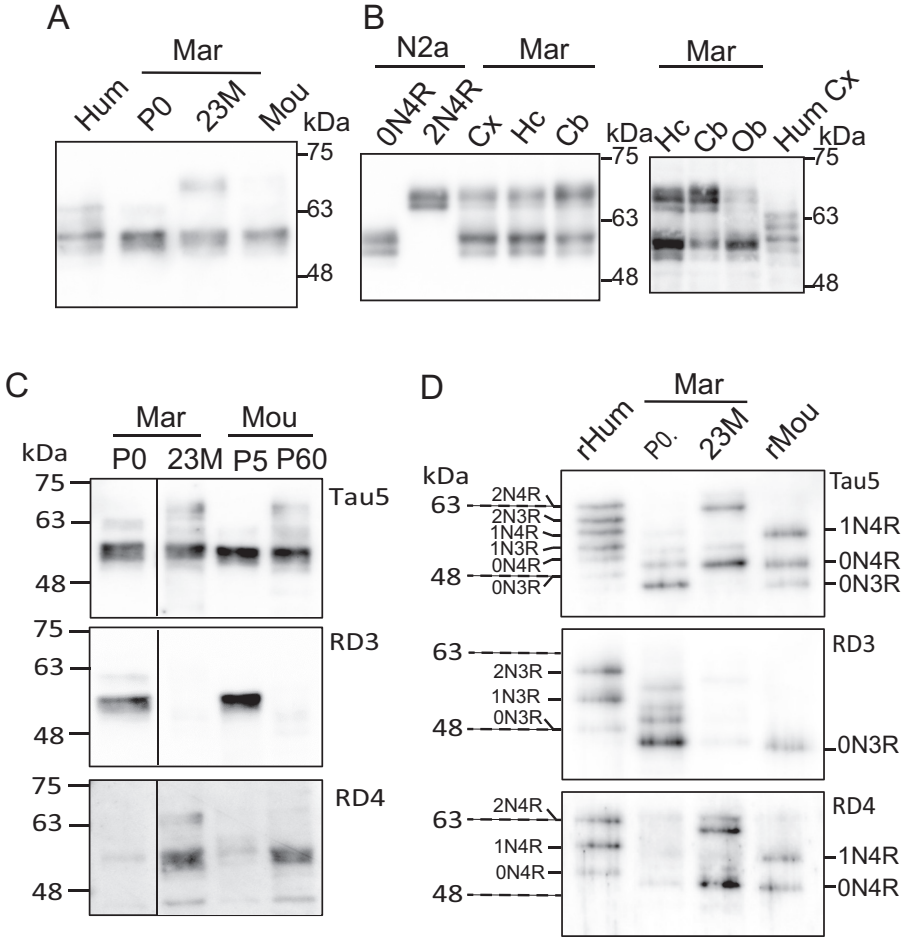

Figure 4. Isoforms of tau protein expressed in marmoset brains. *A*, immunoblot of tau expressed in brains of newborn (*P0*) and adult (23-month (*23M*)) marmosets with the Tau5 antibody denoting total tau. The brain lysate of adult human (*Hum*) and neonatal mouse (*Mou*) is shown in the *left* and *right lane*, respectively. *B*, immunoblot of tau expressed in various brain regions with Tau5. *Left panel*, cerebral cortex (*Cx*), hippocampus (*Hc*), and cerebellum (*Cb*) of a marmoset brain. 0N3R and 2N4R marmoset tau expressed in Neuro-2a cells are run in the *left two columns*. *Right*, hippocampus (*Hc*), cerebellum (*Cb*), and olfactory bulb (*Ob*) and cortex of the human brain (*Hum cx*). *C*, immunoblots of tau expressed in marmoset brains at P0 and 23 months with antibodies specific for 3R tau (*RD3*) or 4R tau (*RD4*). Tau in brains of mice at P5 and in adults (P60) are shown for comparison. Total tau is shown in the *top panel* (Tau5). *D*, immunoblots of dephosphorylated marmoset brain tau with RD3 or RD4. The brain extract of newborn (P0) or adult (23-month) marmosets was dephosphorylated with alkaline phosphatase and immunoblotted with Tau5. Six recombinant isoforms of human tau (*left lane*) and three isoforms of mouse tau are included and *labeled* on *both sides* of the blots, respectively.

The isoforms of tau with different numbers of N-terminal insertions can be distinguished by their electrophoretic mobility on SDS-PAGE. However, phosphorylation affects tau mobility and renders their definite identification difficult. Therefore, we dephosphorylated brain tau by alkaline phosphatase and then subjected it to SDS-PAGE and immunoblotting. To draw comparisons with nonphosphorylated tau, recombinant human (rHum, six isoforms) and mouse (rMou, three isoforms of 0N3R, 0N4R, and 1N4R) tau, which were synthesized in *Escherichia coli*, were used (Fig. 4*D*). The dephosphorylated marmoset tau in adult brains included two sharp bands that were slightly smaller than the human 0N4R and 2N4R isoforms. In contrast, those of the newborn marmoset brain lysate presented one major band close to mouse 0N3R tau and one minor

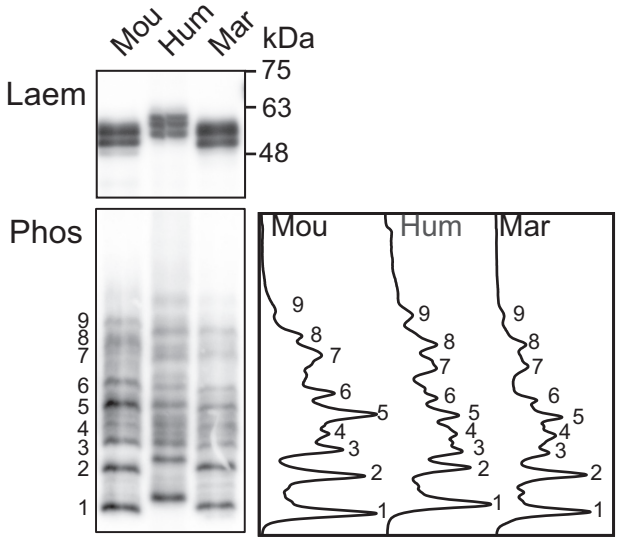

Figure 5. Phosphorylation states of marmoset tau expressed in cultured cells and its comparison with those of human and mouse tau. *Top*, immunoblot of mouse (*Mou*), human (*Hum*), and marmoset (*Mar*) 0N4R tau expressed in Neuro-2a cells with Tau5 after Laemmli's SDS-PAGE. *Bottom*, immunoblot with Tau5 after Phos-tag SDS-PAGE. *Right*, a densitometric scan of bands separated in Phos-tag SDS-PAGE. Bands are *numbered* from the fastest migrating tau, which represents nonphosphorylated tau.

band close to the human 1N3R isoform (Fig. 4*D*). To validate the 3R or 4R isoforms, dephosphorylated tau was reacted with RD3 or RD4 (Fig. 4*D*). The results clearly demonstrate that adult marmoset tau was almost exclusively composed of 4R tau (Fig. 4*D*, *bottom*) and that P0 tau was mainly composed of 3R (Fig. 4*D*, *middle*). We observed weak reactions from RD4 in the P0 lysate, suggesting that a small amount of 4R tau of 0N, 1N, or 2N is expressed in marmoset brains at P0. These results show that 0N3R tau is mainly expressed in newborn marmoset brains and that 0N4R and 2N4R are predominantly expressed in adult marmoset brains.

Marmoset tau can be phosphorylated nearly the same as human or mouse tau when expressed in cultured cells

We have previously shown that Phos-tag SDS-PAGE is powerful for the analysis of the detailed and total phosphorylation of tau by expressing it in culture cell lines (39). The phosphorylation of marmoset tau was compared with that of human or mouse tau exogenously expressed in Neuro-2a cells by immunoblotting with Tau5 after Phos-tag SDS-PAGE (Fig. 5). Marmoset, human, and mouse 0N4R tau appeared as broad bands at a molecular mass of ~55 kDa in Laemmli's SDS-PAGE (Fig. 5, *Laem*). In contrast, marmoset, human, and mouse tau were separated into approximately nine bands with a similar pattern of bands by Phos-tag SDS-PAGE (Fig. 5, *Phos*). Each band represents a distinct phosphoisotype of 0N4R tau with different quantities and sites of phosphorylation (see Fig. 3 in Kimura *et al.* (39)). Densitometric scanning results confirmed that their banding patterns are almost identical, although some minor differences were found, such as the stronger intensity of band 5 in mouse tau (Fig. 5). Thus, marmoset tau can be phosphorylated in Neuro-2a cells at the same sites and to a similar degree as in human or mouse tau, indicating that marmoset tau can be used for the analysis of phosphorylation in place of human tau.

Phosphorylation of tau at AD pathological sites in marmoset brains

We examined the phosphorylation of tau at several AD pathological sites in marmoset brains. We used the anti-phospho-tau antibodies AT8, AT180, and PHF-1, which are typically used for the diagnosis of AD by the immunostaining of NFTs in post-mortem brain sections (12, 13). The *top panel* of Fig. 6*A* is an immunoblot of total tau found in the brain lysates of three marmosets at P0 and in adults. Because mouse tau at P5 is highly phosphorylated, we used it as a positive control of phosphorylation in an immunoreaction (Fig. 6*A*, *left lane*). A normal adult human brain lysate was also run to draw comparisons (Fig. 6*A*, *right lane*). Total tau is shown in the *top* panel with Tau5. Newborn marmoset tau was recognized by the AT8, AT180, and PHF-1 antibodies, although the reactivity was weaker than that observed for neonatal mouse tau. In contrast, adult marmoset and adult human tau did not react with AT8 and AT180. A very faint reaction with PHF-1 was detected from adult marmoset tau but not for adult human tau.

The above listed anti-phospho-tau AD epitopes are generated by double phosphorylation at Ser-202 and Thr-205 for AT8, at Thr-231 and Ser-235 for AT180, and at Ser-396 and Ser-404 for PHF-1 (40). We then examined whether only one or both of the sites are not phosphorylated in adult marmoset brains. In this experiment, the reactivity of adult marmoset tau was compared with that of two adult human brains, whose PMI was 3.2 and 4.36 h, respectively (Fig. 6*B*, *Hum*). For the AT8 site, Ser-202 was phosphorylated in adult marmoset and human tau to almost the same extent, whereas Thr-205 was not phosphorylated. For the AT180 site, Thr-231 and Ser-235 were phosphorylated in marmoset brains, although to a much lesser extent than P5 mouse brain tau, but only a trace reaction was detected from pSer-235 in human brains. At the PHF-1 site, Ser-404 was phosphorylated in both marmoset and human brains with stronger reactions found in human tau, a lesser degree of phosphorylation at Ser-396 was found in marmoset brains, and no phosphorylation was observed in human brains. For quantification, we measured the intensity of the area covering total tau detected with Tau5 (a *bracket* in the *top panel* of Fig. 6*B*), as banding patterns observed in the marmosets and humans differed while also differing slightly among the antibodies used. Ser-202 and Ser-404 were highly phosphorylated at ~60–70% and 45–55% of mouse tau at P5, respectively. Whereas marmoset tau was phosphorylated more than human tau at most sites, Ser-404 alone was more phosphorylated in the human brains than in the marmoset brains. These results describe, for the first time, the biochemical phosphorylation states of tau in marmoset brains.

Discussion

The marmoset is expected to be used as a nonhuman primate model of human neurodegenerative diseases (20, 27). Tauopathies are neurodegenerative diseases found in the brain where hyperphosphorylated tau accumulates (2–4). To use marmosets as a model of tauopathies, it is crucial to determine the nature of marmoset tau, such as its isoform expression and phosphorylation. However, there has thus far been no bio-

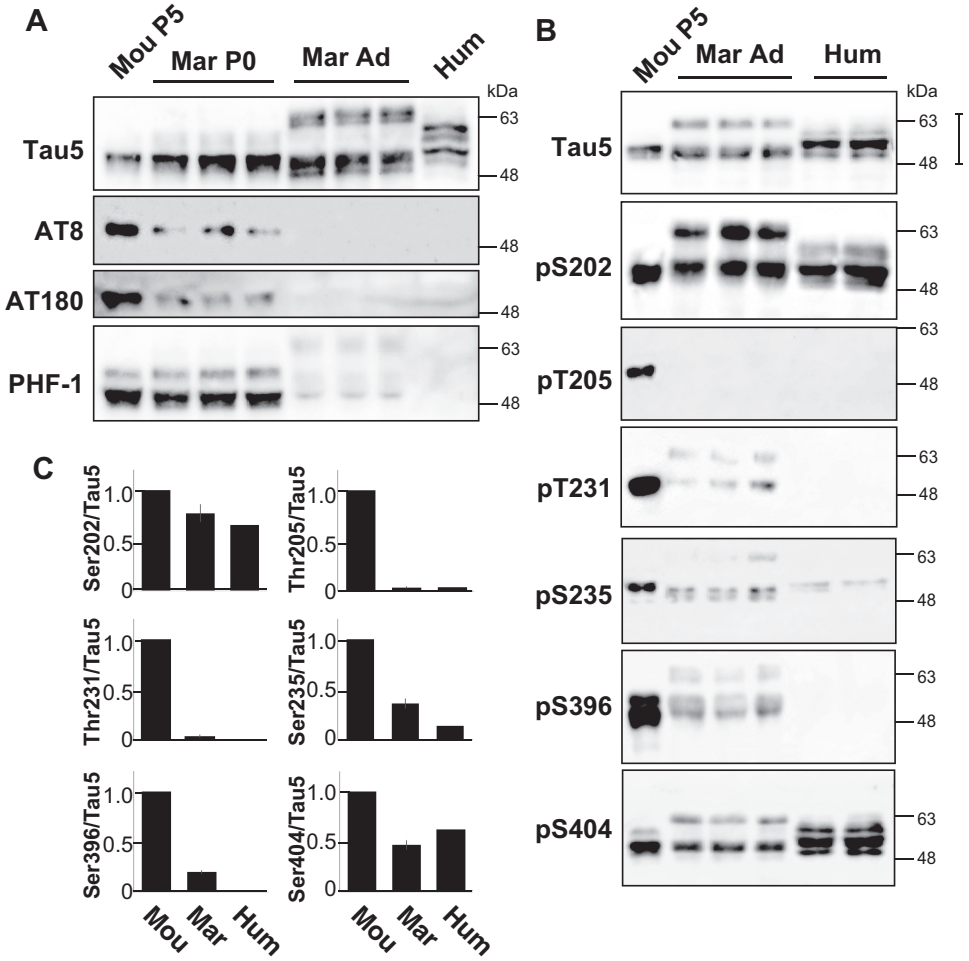

Figure 6. Phosphorylation of tau in the brains of newborn and adult marmosets. *A*, phosphorylation of newborn (three at P0) and adult (three at 1.9, 4.7, and 5.8 years of age) marmoset tau at AD pathological sites, AT8, AT180, and PHF-1. Mouse brain tau at P5 (*left*) and adult human tau (*right*) are shown for comparison. The *top panel* shows the total volume of tau immunoblotted with Tau5. *B*, the site-specific phosphorylation of tau in brains of adult marmosets and humans. An immunoblot of total tau is shown with Tau5 in the *top panel*. The phosphorylation of major (S/T)P phosphorylation sites at Ser-202, Thr-205, Thr-231, Ser-235, Ser-396, or Ser-404 is immunoblotted with respective phosphorylation site-specific antibodies. Mouse tau at P5 is a positive control. A *bracket* on the *top panel* indicates the quantified region. *C*, quantification of phosphorylation at each site examined in *B*. The amount of tau protein was normalized in a blot with Tau5, and phosphorylation is expressed as the ratio to that of mouse tau. *Error bars*, S.D.

chemical analysis of the tau protein found in marmoset brains. Here, we cloned marmoset tau cDNA and investigated the expression of tau isoforms and its phosphorylation. Unexpectedly, we found that marmoset tau did not contain the so-called "primate-unique motif" in the N-terminal region, and the isoform expressed in adult brains was the 4R isoform as found in mouse brains. Adult marmoset tau did not react or reacted very weakly with several anti-pathological phospho-tau antibodies, although brain tissues were removed shortly after sacrifice. Thus, we found that marmoset tau resembles mouse tau rather than human tau in several biochemical aspects.

It was recently proposed that the N-terminal 11 amino acids, which are found in human tau but not rodent tau, reveal a motif unique to primates (35). However, marmoset tau did not contain 10 of the primate-unique 11 amino acids, although the marmoset is a primate. In comparing the N-terminal amino acids of a larger group of primates, including both Old World and New World monkeys and several prosimians, we found that all New World monkeys do not include 10 of the 11 amino acids of the "primate-unique motif." In contrast, prosimians (sifaka and lemur), which separated from anthropoids before the separation of Old and New World monkeys, did contain the motif, suggesting that the deletion took place in New World monkeys after they separated from Old World monkeys. Further, Stefanoska *et al.* (35) note that dog tau is an exception, as it includes this N-terminal motif. However, we found that cat and panda tau also have this sequence, although the motif extends to 14 amino acids in length with an additional 3 amino acids at the N-terminal upstream. Interestingly, tau of the Tasmanian devil, a marsupial animal, contains an additional 15 amino acids with an extra 8 amino acids in the upstream region (Fig. 2*A*). From the phylogenic tree of mammalian tau (Fig. 2*B*), it may be concluded that ancestral mammalian tau contains a certain portion of the amino acid sequence at the N-terminal region, including the origin of the primate-unique motif. Some groups of mammals lost the sequence after their divergence into their respective groups (Fig. 2*B*), such that New World monkeys, rodents, and ungulates might have independently lost the 10, 11, and 12 amino acids. The variability observed in the sequence suggests that this N-terminal region is highly

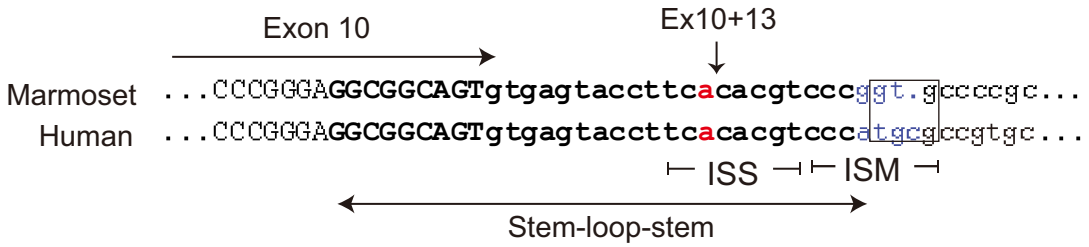

Figure 7. Nucleotide sequence comparison of human and marmoset tau genes around the exon 10 –splicing site. The regions of the stem-loop-stem, ISS (intron-splicing silencer), and ISM (intron-splicing modulator) according to Qian and Liu (43) are indicated. Ex10+13 (*red*) is a site that regulates Exon 10 splicing, which is replaced with guanine in rodent tau. The nucleotide sequence (*blue*) indicated by the *box* differs between marmoset and human tau genes.

changeable in the tau molecule. A question that thus arises concerns whether such variability represents species-specific functions of the N-terminal region in the tau molecule or not.

The isoform expression pattern of tau in marmosets was found to be similar to that of mice rather than humans. It is well-documented that both 3R and 4R isoforms are expressed in adult human brains (21, 22). Other primates, such as chimpanzees and gibbons, also express both 3R and 4R in the adult stage (41). In contrast, 4R tau is exclusively expressed in adult mouse and rat brains (20, 24, 38). Although the marmoset is a primate, only 4R tau is expressed in its adult brain. 3R or 4R tau is generated through the alternative splicing of exon 10. The splicing of exon 10 is regulated by the nucleotide sequence at the 5′ splicing site of exon 10 and in a nucleotide at Ex10+13 in the stem-loop (42, 43). Because marmoset tau includes the same nucleotide sequence in its stem-loop as that found in humans (Fig. 7) (42, 43), the present result was surprising. However, we identified a difference in the nucleotide sequence of the intron-splicing modulator (ISM) region (Fig. 7, *blue* in a *box*). The ISM counteracts the intron-splicing silencer (ISS)-mediated inhibition of the 5′ splicing site (43, 44). The ISM of the marmoset may lose its inhibitory activity, counteracting the inhibitory activity of the ISS. It may be interesting to examine the effects of splicing factor FUS or SFPQ on the splicing of exon 10 of marmoset tau (45). The regulatory mechanism of the splicing of exon 10 is important, as indicated by the fact that the ratio of 4R to 3R increases in AD, whereas the forced decrease in the ratio of 4R to 3R by antisense oligonucleotide ameliorates the occurrence of epilepsy (46).

Marmoset tau differed from that of humans and mice in terms of the N-terminal isoform expression. Splicing in or out of exons 2 and 3 generates 0N, 1N, and 2N isoforms (21, 22). The 1N isoforms of both 3R and 4R tau are most abundantly expressed in adult human brains (9, 47), whereas the 0N isoform is highly expressed in adult mouse brains with a lesser and equal expression of 1N and 2N (20). In contrast, the 0N and, to a lesser extent, 2N isoforms are expressed in adult marmoset brains, whereas the 1N isoform is rarely detected. Although the functions of N-terminal insertions are yet not known, differences in the localization and interacting proteins of tau isoforms have been reported (48, 49), and the 2N isoform interacts with proteins related to neurodegenerative diseases (49). It may be interesting to observe 2N isoform expression in marmoset brain regions to know their possible function or relationship to the diseases.

Phosphorylation is another important property of tau to be considered. Immunohistochemistry has been employed to identify pathological tau phosphorylation in marmoset brains. Two reports on this issue have been published; one report shows that tau is not phosphorylated even in old age using the PHF-1 antibody (50), whereas another recent paper claims that the pathological phosphorylation of tau at Thr-231 commences in the adolescent stage and progressively increases with age (51). Thus, the study of marmoset tau phosphorylation is only at the beginning stage. In this study, we used both antibodies and several other anti-phosphoantibodies in immunoblots to detect phosphorylation of tau. In particular, using the immunoblotting method, we could identify the isoforms of tau expressed in marmoset brains. Further, we used the perinatal mouse tau as a positive control of the phosphorylation to make the analysis more quantitative. We found that both PHF1 and Thr-231 sites were weakly phosphorylated in adult marmoset brains. The results suggest that the previous difference in the immunocytochemical staining could be caused by difference in the sensitivity of the detection.

We first tested whether marmoset tau can be phosphorylated similarly to human tau under the same cellular conditions by expressing these tau proteins in Neuro-2a cells. We used Phos-tag phosphoaffinity SDS-PAGE to observe the overall phosphorylation profile of tau (39). Marmoset tau presented almost the same banding pattern as that of human and mouse tau, indicating that marmoset and human tau are phosphorylated at the same site and to the same extent in cultured cells. This result constitutes important basic information when we consider a particular animal as a model of human tauopathies, but in a strict sense, such information has not been available previously. The present data obtained by Phos-tag indicate that marmoset tau can be substituted for human tau in the analysis of phosphorylation.

There are at least two critical issues to overcome in the study of the *in vivo* phosphorylation of tau in primates. One is dephosphorylation during the PMI. Wang *et al.* (16) reported that the dephosphorylation of tau proceeds quickly during the PMI. As it takes more time to dissect the brains of larger animals after their sacrifice, phosphorylation studies of primate brains are challenging. We perfused marmosets with PBS immediately after sacrifice, followed by the dissection of brains after ~10 min of perfusion. It took ~10–15 min to completely remove various brain regions. However, this time period was considerably shorter than the 3–4-h PMI required for the human brains used to draw comparisons, suggesting that the present data more closely reflect the phosphorylation of tau in primate brains than those reported. Nevertheless, the phosphorylation of adult marmoset tau was low. Interesting sites are Ser-202 and

Ser-404 that were still strongly phosphorylated, although the levels were slightly less than those observed in P5 mouse brains, which were prepared within 1 min following cervical spinal cord dislocation (20). The results suggest resistance of these sites to dephosphorylation during the PMI. This is consistent with our previous observations of slow dephosphorylation at these sites (52, 53) and with other findings that Ser-404 was phosphorylated in 50–60% of tau molecules in adult human brains (14, 54). Tau is physiologically phosphorylated at Ser-202 and Ser-404. Additional phosphorylation at Thr-205 and Ser-396 creates the pathological sites detected by AT8 (Ser-202 and Thr-205) and PHF-1 (Ser-396 and Ser-404) observed in AD. It may be important to clarify the molecular mechanism that induces Thr-205 and/or Ser-396 phosphorylation to understand the mechanisms of abnormal phosphorylation.

Another is the effect of anesthesia, which is an essential treatment of animals prior to the sacrifice. The anesthesia treatment is demonstrated to increase the phosphorylation of tau through hypothermia of animals (18). We used ketamine and pentobarbital to anesthetize marmosets, but the phosphorylation states of marmoset tau thus prepared were relatively low and rather similar to human tau in autopsy samples with 3–4-h PMI. There is a report that investigated tau phosphorylation using human biopsy samples (17), in which tau is highly phosphorylated. Although these data have been thought to represent the phosphorylation states of tau close to that in living brains, there is a possibility that tau in those biopsy samples was phosphorylated highly during the anesthesia at the time of brain surgery. We think our marmoset brain preparation is similar to biopsy of human brains, although marmosets were sacrificed shortly before the brain dissection. Nonetheless, the phosphorylation states were different between them; marmoset tau was low, and biopsy human tau was high. Marmoset tau, which was once highly phosphorylated during anesthesia, might have been dephosphorylated during the dissection process. By minimizing the effects of PMI and anesthesia in the preparation of brains from marmosets, however, we would be able to approach the *in vivo* phosphorylation states of tau in primate brains.

We showed here for the first time that the expression of tau isoforms in marmoset brains differs from that in humans brains but rather resembles that in mouse brains. These results may raise a question about the use of the marmoset as a model of human tauopathies. However, we still think that marmosets are a better model than mouse. There are a number of differences between mouse and marmoset brains. For example, the overall structure of the brain differs between these two species; whereas the striatum of marmoset is separated into caudate nucleus and putamen, these structures are undistinguishable in the mouse (25). The expression patterns of the genes that regulate brain development are different between the mouse and the marmoset, especially in the areas of the brain that have connections to the prefrontal cortex that are presumably involved in higher cognitive functions (55). Further, the long life span of the marmoset, about 16–18 years, compared with ~2 years in rodents, is a big advantage in the study of age-dependent diseases. On the other hand, there would be some limitations, particularly upon using marmosets as a model of tauopathies where both 3R and 4R tau aggregates are involved. Thus, our present results provide useful information on tau proteins in marmosets, which will be used as a model of tauopathy neurodegeneration in the future.

Experimental procedures

Antibodies and chemicals

Anti-tau Tau5, anti-phospho-tau AT8, and anti-phospho-tau AT180 were purchased from Thermo Fisher Scientific (Fremont, CA). Anti-3R tau RD3 and anti-4R tau RD4 were obtained from Millipore (Darmstadt, Germany). Anti-phospho-Thr-205 was obtained from Invitrogen. Anti-phospho-Ser-202, anti-phospho-Thr-231, anti-phospho-Ser-235, anti-phospho-Ser-396, and anti-phospho-Ser-404 were purchased from Abcam (Cambridge, UK). PHF-1 was a kind gift from Dr. Peter Davies at the Feinstein Institute for Medical Research. TauE1 was produced by immunizing rabbits with a peptide of human tau amino acids 20–38 LGDRKDQGGYTMHQDQ-EGD.[5] Phos-tag acrylamide, 4-(2-aminoethyl)-benzenesulfonyl fluoride hydrochloride (AEBSF), and bacterial alkaline phosphatase were purchased from Wako Chemicals (Osaka, Japan). Leupeptin was obtained from the Peptide Institute (Osaka, Japan).

Brain samples

Common marmoset (*C. jacchus*) maintenance and the tissue sample collection were performed at Keio University and the RIKEN Center for Brain Science. Marmoset experiments conducted for this project were approved by the Institutional Animal Care and Use Committees of the RIKEN (approval number H28-2-219(5)), the Keio University Institutional Animal Care and Use Committee (approval number 11006-(3)), and the Research Ethics Committee of Tokyo Metropolitan University (approval number A28-11, A29-21). Animal handling and experimental procedures were performed in accordance with RIKEN's institutional guidelines for the use of laboratory animals, which correspond with Guidelines for Proper Conduct of Animal Experiments of the Science Council of Japan (2006). Animal care was conducted in accordance with recommendations of the Guide for the Care and Use of Laboratory Animals (Institute of Laboratory Animal Resources, 1996). In this study, six common marmosets were used: three newborn marmosets at P0, two adult females of 1 year and 11 months and of 5 years and 7 months, and one adult male of 4 years and 8 months.

For brain tissue preparation, marmosets were anesthetized with ketamine (10 mg/kg) and pentobarbital (80 mg/kg) by intramuscular injection at room temperature around 25 °C. Within 5 min, all marmosets were sacrificed by the incision of the diaphragm, and then after 30 s, they were perfused with PBS at room temperature. After 10 min of perfusion, various brain regions were removed in 25–35 min, immediately frozen in liquid nitrogen, and stored at −80 °C until use.

Human brain tissues were obtained from the brain bank of the Tokyo Metropolitan Institute of Gerontology, and the study

[5] N. Sahara, manuscript in preparation.

was approved by the ethics committees of the Tokyo Metropolitan Institute of Gerontology (approval number Q-No.4 (5/27/2016)) and of Tokyo Metropolitan University (approval number, H28-26, H29-66). We declare that the present studies abide by the Declaration of Helsinki principles. Two individuals were used; a woman who died at the age of 84 years and a man who died at the age 80 years at PMIs of 4.36 and 3.2 h, respectively. The mouse experiments were approved by the Research Ethics Committee of Tokyo Metropolitan University (approval number A28-10, A29-20). C57BL/6J mice were obtained through Sankyo Lab Service (Tokyo, Japan). Brains were removed immediately or within 1 min after sacrifice by cervical dislocation.

Brains and brain tissues were individually homogenized in 10 mM Tris-HCl, pH 7.4, 1 mM EGTA, 0.8 M NaCl, 10% sucrose, 10 mM NaF, 10 mM β-glycerophosphate, 0.4 mM AEBSF, 10 mg/ml leupeptin, and 1 mM DTT. After centrifugation at 15,000 $\times$ *g* for 20 min, the supernatant was used as the brain extract as described previously (39).

For the dephosphorylation experiments, marmoset brains were homogenized in 10 mM Tris-HCl, pH 8.8, 1 mM EGTA, 0.8 M NaCl, 10% sucrose, 0.4 mM AEBSF, 10 mg/ml leupeptin, and 1 mM DTT. The supernatant generated by centrifugation at 15,000 $\times$ *g* for 20 min was incubated with alkaline phosphatase as described previously (39).

Isolation of tau cDNA from marmoset brains

Total RNA was isolated from marmoset brain cortexes on P0 or after 23 months using ISOGEN (Nippon Gene, catalog no. 315-02504) according to the manufacturer's instructions. cDNA libraries were generated by the reverse transcription of mRNA using the Superscript III First-Strand synthesis system (Invitrogen, catalog no. 18080-051) with oligo(dT) as a primer. Marmoset tau cDNA was amplified by PCR while using the cDNA library as a template. Primers included 5′ and 3′ ends of marmoset tau DNA sequences tagged with a restriction enzyme site, an EcoRI site at the 5′ end of the forward primer, and an XbaI site at the 3′ end of the reverse primer; 5′-GAGCACAGAATTCATGGCTGAGCCCCGC-3′ and 5′-CGCTTATCTAGATCACAAACCCTGCTTGGCC-3′ were used as forward and reverse primers, respectively.

PCR was performed using PfuUltra High-Fidelity DNA polymerase (Agilent Technologies, Santa Clara, CA). PCR products were inserted into pcDNA3.1A-Myc-His (+) after digestion at EcoRI and XbaI sites. DNA sequences were analyzed using an ABI 3130 sequencer (Applied Biosystems, Foster City, CA).

RT-PCR for the analysis of tau mRNA in marmoset brains

Tau transcripts in marmoset brains were analyzed by RT-PCR using the cDNA libraries described above and using primers flanking exons 2/3 or exon 10 of marmoset tau cDNA. Two sets of primers were prepared for exons 2/3 and 10. Primers used include the following: exons 2/3, forward 1, 5′-CGCCAGGAGTTCAATGTGATGG-3′ (13–34 bp); exons 2/3, forward 2, GTGACACAGACACTGGCCTGA (80–100 bp); exons 2/3, reverse 1, 5′-ACCAGAGCTAGGTGGTGTCTTTG-3′ (506–528 bp); exons 2/3, reverse 2, 5-TGTCATCGCCTCCAGTCCC-3′ (370–388 bp); exon 10, forward 1, 5′-GTACTCCACCCAAGTCGCCATC-3′ (659–680 bp); exon 10, forward 2, 5′-CGGTTCCACTGAGAACCTGAAG-3′ (750–771 bp); exon 10, reverse 1, 5′-CACGGAAGGTCAGCTTGTGG-3′ (1089–1108 bp); exon 10, reverse 2, 5′-GAGCCACACTTGGAGGTCAC-3′ (922–941 bp).

RT-PCR was performed using GoTaq Green Master mix (Promega, Madison, WI). The expression of exons 2 and 3 or exon 10 was determined by the size of PCR products on electrophoresis using cloned marmoset cDNA as markers.

Expression of tau in Neuro-2a cells

Neuro-2a cells were obtained from the JCRB Cell Bank (Osaka, Japan) and were maintained in minimum essential medium (Thermo Fisher Scientific) supplemented with 10% fetal bovine serum (Biowest, Riverside, MO), 1% nonessential amino acids (Wako, Osaka, Japan), 50 IU/ml penicillin, and 50 μg/ml streptomycin as described previously (56). Neuro-2a cells were transfected with pcDNA3.1 encoding tau cDNA using Lipofectamine 2000 (Invitrogen) according to the manufacturer's instructions.

SDS-PAGE and immunoblotting

SDS-PAGE was performed with 12.5% polyacrylamide gels. Phos-tag SDS-PAGE was performed with 10% polyacrylamide gels containing 50 μM Phos-tag and 100 μM $MnCl_2$ as described previously (39). Immunoblotting was performed as described previously (20).

Bioinformatics

Amino acid sequences of tau were deduced from the protein-coding nucleotide sequence of the mammalian species in the Ensemble genome browser registered as MAPT-210 for humans; MAPT-201s for the chimpanzee, gorilla, orangutan, squirrel monkey, capuchin, night monkey, sifaka, mouse lemur, dog, cat, panda, mouse, and Tasmanian devil; ENSMMUT00000005853 for the macaque; ENSPANT-00000056619 for the olive baboon; MAPT-202s for the gibbon and goat; 204 for the rat; and 205 for the cow. The alignment of the N-terminal 50 amino acid sequences of tau was performed by MEGA7 (57) with ClustalW using the following parameters: pairwise alignment, gap opening penalty = 5 and gap extension penalty = 0.1; multiple alignment, gap opening penalty = 5 and gap extension penalty = 0.1 (57). A phylogenetic tree was constructed in MEGA7 using the neighbor-joining method for the N-terminal 120-amino acid sequence of tau (58). The evolutionary distances were computed using the Poisson correction method (59) and are shown as the number of amino acid substitutions per site. The Poisson correction distance assumes the equality of substitution rates among sites and equal amino acid frequencies while correcting for multiple substitutions at the same site. The rate of variation among sites was modeled with a γ distribution (shape parameter = 1). The optimal tree with the branch length sum = 1.13109959 is shown. The percentage of replicate trees in which the associated taxa clustered together during the bootstrap test (1000 replicates) is shown next to the branches (60).

Author contributions—G. Sharma, T. K., T. S., M. H., G. Sobue, H. O., and S.-i. H. conceptualization; G. Sharma, T. K., S. S., R. K., N. S., M. I., S. I., T. S., K. A., S. M., and M. H. resources; G. Sharma, A. H., S. S., R. K., N. S., M. I., S. I., S. M., and M. H. data curation; G. Sharma, A. H., T. K., S. S., N. S., M. I., K. A., G. Sobue, H. O., and S.-i. H. formal analysis; G. Sharma, A. H., R. K., N. S., M. I., S. I., and T. S. investigation; G. Sharma, A. H., T. K., R. K., M. I., M. H., and S.-i. H. methodology; G. Sharma and S.-i. H. writing-original draft; T. K., S. S., M. I., S. I., and K. A. validation; S. S., R. K., N. S., M. I., K. A., S. M., M. H., G. Sobue, and H. O. writing-review and editing; T. S., K. A., G. Sobue, and S.-i. H. project administration; G. Sobue, H. O., and S.-i. H. supervision; S.-i. H. funding acquisition.

Acknowledgments—We thank Dr. Aya Takahashi (Tokyo Metropolitan University) for comments on bioinformatics methodology and Dr. Jonna Swanson (Tokyo Metropolitan University) for editing the manuscript.

References

1. Arendt, T., Stieler, J. T., and Holzer, M. (2016) Tau and tauopathies. *Brain Res. Bull.* **126,** 238–292 CrossRef Medline
2. Ballatore, C., Lee, V. M., and Trojanowski, J. Q. (2007) Tau-mediated neurodegeneration in Alzheimer's disease and related disorders. *Nat. Rev. Neurosci.* **8,** 663–672 CrossRef Medline
3. Spillantini, M. G., and Goedert, M. (2013) Tau pathology and neurodegeneration. *Lancet Neurol.* **12,** 609–622 CrossRef Medline
4. Wang, Y., and Mandelkow, E. (2016) Tau in physiology and pathology. *Nat. Rev. Neurosci.* **17,** 5–21 CrossRef Medline
5. Goode, B. L., and Feinstein, S. C. (1994) Identification of a novel microtubule binding and assembly domain in the developmentally regulated inter-repeat region of tau. *J. Cell Biol.* **124,** 769–782 CrossRef Medline
6. Hanger, D. P., Anderton, B. H., and Noble, W. (2009) Tau phosphorylation: the therapeutic challenge for neurodegenerative disease. *Trends Mol. Med.* **15,** 112–119 CrossRef Medline
7. Kimura, T., Sharma, G., Ishiguro, K., and Hisanaga, S. I. (2018) Phospho-tau bar code: analysis of phosphoisotypes of tau and its application to tauopathy. *Front. Neurosci.* **12,** 44 CrossRef Medline
8. Brion, J. P., Smith, C., Couck, A. M., Gallo, J. M., and Anderton, B. H. (1993) Developmental changes in tau phosphorylation: fetal tau is transiently phosphorylated in a manner similar to paired helical filament-tau characteristic of Alzheimer's disease. *J. Neurochem.* **61,** 2071–2080 CrossRef Medline
9. Goedert, M., Jakes, R., Crowther, R. A., Six, J., Lübke, U., Vandermeeren, M., Cras, P., Trojanowski, J. Q., and Lee, V. M. (1993) The abnormal phosphorylation of tau protein at Ser-202 in Alzheimer disease recapitulates phosphorylation during development. *Proc. Natl. Acad. Sci. U.S.A.* **90,** 5066–5070 CrossRef Medline
10. Kenessey, A., and Yen, S. H. (1993) The extent of phosphorylation of fetal tau is comparable to that of PHF-tau from Alzheimer paired helical filaments. *Brain Res.* **629,** 40–46 CrossRef Medline
11. Morishima-Kawashima, M., Hasegawa, M., Takio, K., Suzuki, M., Yoshida, H., Titani, K., and Ihara, Y. (1995) Proline-directed and non-proline-directed phosphorylation of PHF-tau. *J. Biol. Chem.* **270,** 823–829 CrossRef Medline
12. Murayama, S., and Saito, Y. (2004) Neuropathological diagnostic criteria for Alzheimer's disease. *Neuropathology* **24,** 254–260 CrossRef Medline
13. Shiarli, A. M., Jennings, R., Shi, J., Bailey, K., Davidson, Y., Tian, J., Bigio, E. H., Ghetti, B., Murrell, J. R., Delisle, M. B., Mirra, S., Crain, B., Zolo, P., Arima, K., Iseki, E., *et al.* (2006) Comparison of extent of tau pathology in patients with frontotemporal dementia with Parkinsonism linked to chromosome 17 (FTDP-17), frontotemporal lobar degeneration with Pick bodies and early onset Alzheimer's disease. *Neuropathol. Appl. Neurobiol.* **32,** 374–387 CrossRef Medline
14. Kimura, T., Hatsuta, H., Masuda-Suzukake, M., Hosokawa, M., Ishiguro, K., Akiyama, H., Murayama, S., Hasegawa, M., and Hisanaga, S. (2016) The abundance of nonphosphorylated tau in mouse and human tauopathy brains revealed by the use of Phos-Tag method. *Am. J. Pathol.* **186,** 398–409 CrossRef Medline
15. Kinoshita, E., Kinoshita-Kikuta, E., Takiyama, K., and Koike, T. (2006) Phosphate-binding tag, a new tool to visualize phosphorylated proteins. *Mol. Cell Proteomics* **5,** 749–757 CrossRef Medline
16. Wang, Y., Zhang, Y., Hu, W., Xie, S., Gong, C. X., Iqbal, K., and Liu, F. (2015) Rapid alteration of protein phosphorylation during postmortem: implication in the study of protein phosphorylation. *Sci. Rep.* **5,** 15709 CrossRef Medline
17. Matsuo, E. S., Shin, R. W., Billingsley, M. L., Van deVoorde, A., O'Connor, M., Trojanowski, J. Q., and Lee, V. M. (1994) Biopsy-derived adult human brain tau is phosphorylated at many of the same sites as Alzheimer's disease paired helical filament tau. *Neuron* **13,** 989–1002 CrossRef Medline
18. Whittington, R. A., Bretteville, A., Dickler, M. F., and Planel, E. (2013) Anesthesia and tau pathology. *Prog. Neuropsychopharmacol. Biol. Psychiatry* **47,** 147–155 CrossRef Medline
19. Yu, Y., Run, X., Liang, Z., Li, Y., Liu, F., Liu, Y., Iqbal, K., Grundke-Iqbal, I., and Gong, C. X. (2009) Developmental regulation of tau phosphorylation, tau kinases, and tau phosphatases. *J. Neurochem.* **108,** 1480–1494 CrossRef Medline
20. Tuerde, D., Kimura, T., Miyasaka, T., Furusawa, K., Shimozawa, A., Hasegawa, M., Ando, K., and Hisanaga, S. I. (2018) Isoform-independent and -dependent phosphorylation of microtubule-associated protein tau in mouse brain during postnatal development. *J. Biol. Chem.* **293,** 1781–1793 CrossRef Medline
21. Goedert, M., Spillantini, M. G., Potier, M. C., Ulrich, J., and Crowther, R. A. (1989) Cloning and sequencing of the cDNA encoding an isoform of microtubule-associated protein tau containing four tandem repeats: differential expression of tau protein mRNAs in human brain. *EMBO J.* **8,** 393–399 CrossRef Medline
22. Kosik, K. S., Orecchio, L. D., Bakalis, S., and Neve, R. L. (1989) Developmentally regulated expression of specific tau sequences. *Neuron* **2,** 1389–1397 CrossRef Medline
23. Takuma, H., Arawaka, S., and Mori, H. (2003) Isoforms changes of tau protein during development in various species. *Brain Res. Dev. Brain Res.* **142,** 121–127 CrossRef Medline
24. McMillan, P., Korvatska, E., Poorkaj, P., Evstafjeva, Z., Robinson, L., Greenup, L., Leverenz, J., Schellenberg, G. D., and D'Souza, I. (2008) Tau isoform regulation is region- and cell-specific in mouse brain. *J. Comp. Neurol.* **511,** 788–803 CrossRef Medline
25. Izpisua Belmonte, J. C., Callaway, E. M., Caddick, S. J., Churchland, P., Feng, G., Homanics, G. E., Lee, K. F., Leopold, D. A., Miller, C. T., Mitchell, J. F., Mitalipov, S., Moutri, A. R., Movshon, J. A., Okano, H., Reynolds, J. H., *et al.* (2015) Brains, genes, and primates. *Neuron* **86,** 617–631 CrossRef Medline
26. The Marmoset Genome Sequencing and Analysis Consortium (2014) The common marmoset genome provides insight into primate biology and evolution. *Nat. Genet.* **46,** 850–857 CrossRef Medline
27. Okano, H., Hikishima, K., Iriki, A., and Sasaki, E. (2012) The common marmoset as a novel animal model system for biomedical and neuroscience research applications. *Semin. Fetal Neonatal Med.* **17,** 336–340 CrossRef Medline
28. Sasaki, E., Suemizu, H., Shimada, A., Hanazawa, K., Oiwa, R., Kamioka, M., Tomioka, I., Sotomaru, Y., Hirakawa, R., Eto, T., Shiozawa, S., Maeda, T., Ito, M., Ito, R., Kito, C., *et al.* (2009) Generation of transgenic non-human primates with germline transmission. *Nature* **459,** 523–527 CrossRef Medline
29. Yun, J. W., Ahn, J. B., and Kang, B. C. (2015) Modeling Parkinson's disease in the common marmoset (*Callithrix jacchus*): overview of models, methods, and animal care. *Lab. Anim. Res.* **31,** 155–165 CrossRef Medline
30. Kobayashi, R., Takahashi-Fujigasaki, J., Shiozawa, S., Hara-Miyauchi, C., Inoue, T., Okano, H. J., Sasaki, E., and Okano, H. (2016) α-Synuclein aggregation in the olfactory bulb of middle-aged common marmoset. *Neurosci. Res.* **106,** 55–61 CrossRef Medline
31. Shimozawa, A., Ono, M., Takahara, D., Tarutani, A., Imura, S., Masuda-Suzukake, M., Higuchi, M., Yanai, K., Hisanaga, S. I., and Hasegawa, M.

(2017) Propagation of pathological α-synuclein in marmoset brain. *Acta Neuropathol. Commun.* **5,** 12 CrossRef Medline
32. Couchie, D., Mavilia, C., Georgieff, I. S., Liem, R. K., Shelanski, M. L., and Nunez, J. (1992) Primary structure of high molecular weight tau present in the peripheral nervous system. *Proc. Natl. Acad. Sci. U.S.A.* **89,** 4378–4381 CrossRef Medline
33. Goedert, M., Spillantini, M. G., and Crowther, R. A. (1992) Cloning of a big tau microtubule-associated protein characteristic of the peripheral nervous system. *Proc. Natl. Acad. Sci. U.S.A.* **89,** 1983–1987 CrossRef Medline
34. Forrest, S. L., Kril, J. J., Stevens, C. H., Kwok, J. B., Hallupp, M., Kim, W. S., Huang, Y., McGinley, C. V., Werka, H., Kiernan, M. C., Götz, J., Spillantini, M. G., Hodges, J. R., Ittner, L. M., and Halliday, G. M. (2018) Retiring the term FTDP-17 as MAPT mutations are genetic forms of sporadic frontotemporal tauopathies. *Brain* **141,** 521–534 CrossRef Medline
35. Stefanoska, K., Volkerling, A., Bertz, J., Poljak, A., Ke, Y. D., Ittner, L. M., and Ittner, A. (2018) An N-terminal motif unique to primate tau enables differential protein-protein interactions. *J. Biol. Chem.* **293,** 3710–3719 CrossRef Medline
36. Meredith, R. W., Hekkala, E. R., Amato, G., and Gatesy, J. (2011) A phylogenetic hypothesis for Crocodylus (Crocodylia) based on mitochondrial DNA: evidence for a trans-Atlantic voyage from Africa to the New World. *Mol. Phylogenet. Evol.* **60,** 183–191 CrossRef Medline
37. Rogers, J., and Gibbs, R. A. (2014) Comparative primate genomics: emerging patterns of genome content and dynamics. *Nat. Rev. Genet.* **15,** 347–359 CrossRef Medline
38. Bullmann, T., Härtig, W., Holzer, M., and Arendt, T. (2010) Expression of the embryonal isoform (0N/3R) of the microtubule-associated protein tau in the adult rat central nervous system. *J. Comp. Neurol.* **518,** 2538–2553 CrossRef Medline
39. Kimura, T., Hosokawa, T., Taoka, M., Tsutsumi, K., Ando, K., Ishiguro, K., Hosokawa, M., Hasegawa, M., and Hisanaga, S. (2016) Quantitative and combinatory determination of *in situ* phosphorylation of tau and its FTDP-17 mutants. *Sci. Rep.* **6,** 33479 CrossRef Medline
40. Gratuze, M., El Khoury, N. B., Turgeon, A., Julien, C., Marcouiller, F., Morin, F., Whittington, R. A., Marette, A., Calon, F., and Planel, E. (2017) Tau hyperphosphorylation in the brain of ob/ob mice is due to hypothermia: importance of thermoregulation in linking diabetes and Alzheimer's disease. *Neurobiol. Dis.* **98,** 1–8 CrossRef Medline
41. Holzer, M., Craxton, M., Jakes, R., Arendt, T., and Goedert, M. (2004) Tau gene (MAPT) sequence variation among primates. *Gene* **341,** 313–322 CrossRef Medline
42. Grover, A., Houlden, H., Baker, M., Adamson, J., Lewis, J., Prihar, G., Pickering-Brown, S., Duff, K., and Hutton, M. (1999) 5′ splice site mutations in tau associated with the inherited dementia FTDP-17 affect a stem-loop structure that regulates alternative splicing of exon 10. *J. Biol. Chem.* **274,** 15134–15143 CrossRef Medline
43. Qian, W., and Liu, F. (2014) Regulation of alternative splicing of tau exon 10. *Neurosci. Bull.* **30,** 367–377 CrossRef Medline
44. D'Souza, I., and Schellenberg, G. D. (2000) Determinants of 4-repeat tau expression: coordination between enhancing and inhibitory splicing sequences for exon 10 inclusion. *J. Biol. Chem.* **275,** 17700–17709 CrossRef Medline
45. Ishigaki, S., Fujioka, Y., Okada, Y., Riku, Y., Udagawa, T., Honda, D., Yokoi, S., Endo, K., Ikenaka, K., Takagi, S., Iguchi, Y., Sahara, N., Takashima, A., Okano, H., Yoshida, M., *et al.* (2017) Altered Tau isoform ratio caused by loss of FUS and SFPQ function leads to FTLD-like phenotypes. *Cell Rep.* **18,** 1118–1131 CrossRef Medline
46. Schoch, K. M., DeVos, S. L., Miller, R. L., Chun, S. J., Norrbom, M., Wozniak, D. F., Dawson, H. N., Bennett, C. F., Rigo, F., and Miller, T. M. (2016) Increased 4R-tau induces pathological changes in a human-tau mouse model. *Neuron* **90,** 941–947 CrossRef Medline
47. Hong, M., Zhukareva, V., Vogelsberg-Ragaglia, V., Wszolek, Z., Reed, L., Miller, B. I., Geschwind, D. H., Bird, T. D., McKeel, D., Goate, A., Morris, J. C., Wilhelmsen, K. C., Schellenberg, G. D., Trojanowski, J. Q., and Lee, V. M. (1998) Mutation-specific functional impairments in distinct tau isoforms of hereditary FTDP-17. *Science* **282,** 1914–1917 CrossRef Medline
48. Liu, C., and Götz, J. (2013) Profiling murine tau with 0N, 1N and 2N isoform-specific antibodies in brain and peripheral organs reveals distinct subcellular localization, with the 1N isoform being enriched in the nucleus. *PLoS One* **8,** e84849 CrossRef Medline
49. Liu, C., Song, X., Nisbet, R., and Götz, J. (2016) Co-immunoprecipitation with tau isoform-specific antibodies reveals distinct protein interactions and highlights a putative role for 2N tau in disease. *J. Biol. Chem.* **291,** 8173–8188 CrossRef Medline
50. Geula, C., Nagykery, N., and Wu, C. K. (2002) Amyloid-β deposits in the cerebral cortex of the aged common marmoset (*Callithrix jacchus*): incidence and chemical composition. *Acta Neuropathol.* **103,** 48–58 CrossRef Medline
51. Rodriguez-Callejas, J. D., Fuchs, E., and Perez-Cruz, C. (2016) Evidence of Tau hyperphosphorylation and dystrophic microglia in the common marmoset. *Front. Aging Neurosci.* **8,** 315 CrossRef Medline
52. Yotsumoto, K., Saito, T., Asada, A., Oikawa, T., Kimura, T., Uchida, C., Ishiguro, K., Uchida, T., Hasegawa, M., and Hisanaga, S. (2009) Effect of Pin1 or microtubule binding on dephosphorylation of FTDP-17 mutant Tau. *J. Biol. Chem.* **284,** 16840–16847 CrossRef Medline
53. Kimura, T., Tsutsumi, K., Taoka, M., Saito, T., Masuda-Suzukake, M., Ishiguro, K., Plattner, F., Uchida, T., Isobe, T., Hasegawa, M., and Hisanaga, S. (2013) Isomerase Pin1 stimulates dephosphorylation of tau protein at cyclin-dependent kinase (Cdk5)-dependent Alzheimer phosphorylation sites. *J. Biol. Chem.* **288,** 7968–7977 CrossRef Medline
54. Watanabe, A., Hasegawa, M., Suzuki, M., Takio, K., Morishima-Kawashima, M., Titani, K., Arai, T., Kosik, K. S., and Ihara, Y. (1993) *In vivo* phosphorylation sites in fetal and adult rat tau. *J. Biol. Chem.* **268,** 25712–25717 Medline
55. Mashiko, H., Yoshida, A. C., Kikuchi, S. S., Niimi, K., Takahashi, E., Aruga, J., Okano, H., and Shimogori, T. (2012) Comparative anatomy of marmoset and mouse cortex from genomic expression. *J. Neurosci.* **32,** 5039–5053 CrossRef Medline
56. Sharma, G., Tsutsumi, K., Saito, T., Asada, A., Ando, K., Tomomura, M., and Hisanaga, S. I. (2016) Kinase activity of endosomal kinase LMTK1A regulates its cellular localization and interactions with cytoskeletons. *Genes Cells* **21,** 1080–1094 CrossRef Medline
57. Kumar, S., Stecher, G., and Tamura, K. (2016) MEGA7: molecular evolutionary genetics analysis version 7.0 for bigger datasets. *Mol. Biol. Evol.* **33,** 1870–1874 CrossRef Medline
58. Saitou, N., and Nei, M. (1987) The neighbor-joining method: a new method for reconstructing phylogenetic trees. *Mol. Biol. Evol.* **4,** 406–425 CrossRef Medline
59. Zuckerkandl, E., and Pauling, L. (1965) Molecules as documents of evolutionary history. *J. Theor. Biol.* **8,** 357–366 CrossRef Medline
60. Felsenstein, J. (1985) Confidence limits on phylogenies: an approach using the bootstrap. *Evolution* **39,** 783–791 CrossRef Medline